Search for the chiral magnetic wave at STAR with isobar (Ru/Zr) and Au+Au collisions

Ankita Nain[1,*] for the STAR Collaboration

[1]Department of Physics, D.A.V. College, Panjab University, Chandigarh, 160010, India

Abstract. We present the energy dependence of the Chiral Magnetic Wave (CMW) observable in Au+Au collisions from the BES-II higher statistics data at $\sqrt{s_{NN}}$ = 7.7, 19.6, 27 and 200 GeV. The results from participant and spectator event planes are compared to investigate the elliptic flow background in the CMW observable. The normalized difference between positive and negative charged particles of the covariance between v_n and $A_{\rm ch}$ which quantifies the CMW strength for v_2 (signal + background) and v_3 (background only), are presented in Au+Au collisions at 200 GeV. In addition, we report a search for the expected enhancement of the CMW signal in $^{96}_{44}$Ru +$^{96}_{44}$ Ru collisions compared with $^{96}_{40}$Zr +$^{96}_{40}$ Zr collisions at 200 GeV.

1 Introduction

The CMW arises due to coupling between two fundamental quantum phenomena: the Chiral Magnetic Effect (CME) [1, 2], where a chirality imbalance generates an electric current parallel to the magnetic field, and the Chiral Separation Effect (CSE) [3], where an electric charge imbalance induces an axial current along the magnetic field direction. The interplay between these two effects induces an oscillatory propagation of electric and chiral charge densities, leading to a long-wavelength collective excitation known as the Chiral Magnetic Wave (CMW) [4–6]. The CMW induces an electric quadrupole moment in the QGP, where the "poles" ("equator") of the produced fireball acquire additional positive (negative) charge, resulting in difference between elliptic flow of positively and negatively charged particles which is proportional to charge asymmetry ($A_{\rm ch}$) [5, 7]

$$\Delta v_2 = v_2^- - v_2^+ \approx r_2 A_{\rm ch} \tag{1}$$

where $A_{\rm ch} = (\mathrm{N}_+ - \mathrm{N}_-)/(\mathrm{N}_+ + \mathrm{N}_-)$ with N_+ (N_-) denoting the number of positive (negative) charge particles in a given event, while "r_2" is the slope of Δv_2 versus $A_{\rm ch}$ and encodes the strength of the electric quadrupole due to the CMW. Another observable studied is the covariance between $v_n^\pm$ and $A_{\rm ch}$, expressed as $\langle v_n^\pm A_{\rm ch}\rangle - \langle v_n^\pm\rangle\langle A_{\rm ch}\rangle$ commonly referred to as the three-particle integral correlator [8]. The integral covariance difference between the negative and positive charged particles, can be used to determine CMW strength, which can be written as:

$$\Delta \mathrm{IC} = (\langle v_n^- A_{\rm ch}\rangle - \langle v_n^-\rangle\langle A_{\rm ch}\rangle) - (\langle v_n^+ A_{\rm ch}\rangle - \langle v_n^+\rangle\langle A_{\rm ch}\rangle). \tag{2}$$

*e-mail: nainankita55555@gmail.com

Here the angular bracket denotes the average over the events. It is more robust against efficiency corrections and statistical fluctuations, as the sample does not need to be divided into further $A_{\rm ch}$ bins to calculate slope of Δv_2 versus $A_{\rm ch}$. There is substantial evidence that background sources, such as local charge conservation (LCC) significantly affect the experimental measurements. LCC affects charge-dependent flow by creating a net charge asymmetry correlated with flow, mimicking a CMW signal. The following sections address efforts to disentangle the potential CMW signal from background contributions.

2 Analysis Details and Results

We have analyzed minimum-bias events from Au+Au collisions at $\sqrt{s_{NN}}$ = 7.7, 19.6 and 27 GeV recorded by the STAR experiment during the Beam Energy Scan Phase-II (BES-II) at RHIC, along with Au+Au collisions at $\sqrt{s_{NN}}$ =200 GeV collected during 2016 and isobar collisions ($^{96}_{44}$Ru +$^{96}_{44}$ Ru and $^{96}_{40}$Zr +$^{96}_{40}$ Zr) at $\sqrt{s_{NN}}$ =200 GeV. Events are selected with primary vertex position along z direction, within $|V_z| < 70$ cm for BES-II data, $|V_z| <$ 30 cm for 200 GeV Au+Au collisions, and $-35 < V_z < 25$ cm for isobar collisions, with the transverse vertex position within 2 cm of the beam axis. The wider BES-II data vertex cut accommodates broader distributions from less-focused beams, while asymmetric cut for isobars correct for VPD east and west timing offsets that shift the vertex distribution. Tracks are required to have pseudorapidity range of $|\eta| < 1$ and distance of closest approach (DCA) to the primary vertex smaller than 3 cm.

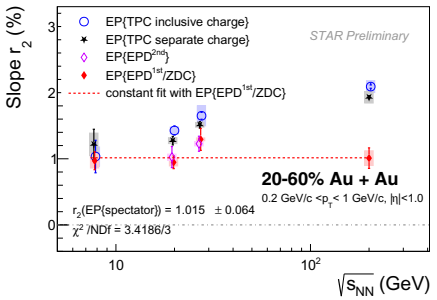

Figure 1. The slope parameter (r_2) as a function of collision energy employing participant and spectator planes.

2.1 Energy dependence of CMW observable in Au+Au collisions

To investigate the slope parameter r_2, that is sensitive to CMW strength, and measure with respect to the spectator and participant event planes, and to explore the low-energy regime where the prerequisites for the CMW may change, we utilize the higher statistics BES-II data, which provides improved resolution for event-plane determination. Table I lists different detectors (TPC, EPD and ZDC) used to determine event planes (EP) using spectators/participants. Figure 1 shows r_2 as a function of center of mass energy, measured using

Table 1. Event-plane detectors and η coverage used at different beam energies.

$\sqrt{s_{NN}}$	7.7 GeV	19.6 GeV	27 GeV	200 GeV
EP$^{\rm 2nd}$ {TPC} (Participant plane)	$\|\eta\| < 1.0$ (Sub-event plane with η gap = 0.3)			
EP$^{\rm 2nd}$ {EPD} (Participant plane)	—	$\|\eta\| < 3.0$	$\|\eta\| < 3.4$	—
EP$^{\rm 1st}$ {EPD} (Spectator plane)	$\|\eta\| > 2.3$	$\|\eta\| > 3.2$	$\|\eta\| > 3.8$	—
EP$^{\rm 1st}$ {ZDC} (Spectator plane)	—	—	—	$\|\eta\| > 6.3$

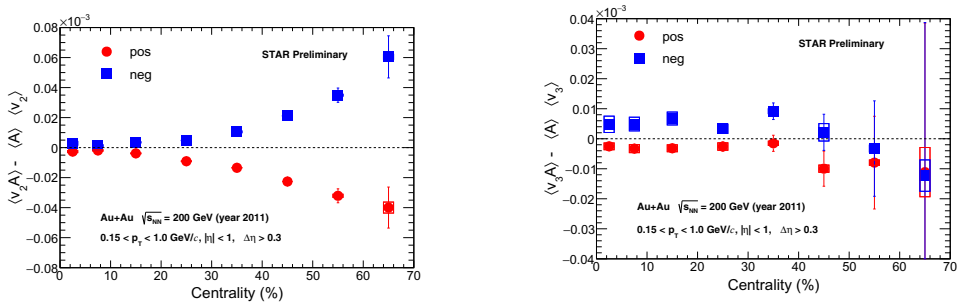

Figure 2. Covariance between v_2 and $A_{\rm ch}$ (Left) and between v_3 and $A_{\rm ch}$ (Right) as a function of collision centrality in Au+Au collisions at $\sqrt{s_{NN}}$ = 200 GeV.

spectator and participant event planes in Au+Au collisions at $\sqrt{s_{NN}}$ = 7.7, 19.6, 27 and 200 GeV. To assess the impact of trivial non-flow autocorrelation effects [9], r_2 is extracted using two methods: one utilizes all charged particles for event plane determination, while the other constructs the event plane from particles having opposite charge to that of the particle of interest. The consistency between these two approaches (Fig. 1) across all energies indicates negligible bias from autocorrelation effects. The spectator-defined event plane is expected to exhibit a stronger correlation from the CMW, while the large pseudo-rapidity gap between the particles of interest effectively reduces non-flow contributions. No notable enhancement in r_2 is observed with energy using the spectator event plane, and the values remain nearly constant across energies, including at 7.7 GeV, where hadronic interactions could become more important. These observations suggest that the observable is mainly influenced by background effects, consistent with the interpretation that the measured correlations arise predominantly from background rather than a genuine CMW signal.

2.2 Comparison of v_2 -$A_{\rm ch}$ and v_3-$A_{\rm ch}$ covariances in Au+Au collisions

It is predicted that backgrounds such as local charge conservation (LCC) which qualitatively account for a finite r_2, also generate a similar effect on r_3 (manifested as the slope of Δv_3 versus $A_{\rm ch}$) [10]. We therefore examine the v_3 -$A_{\rm ch}$ correlation to assess background contributions. Figure 2 (left) presents the covariance between v_2 and $A_{\rm ch}$ as a function of collision centrality in Au+Au collisions at $\sqrt{s_{NN}}$ = 200 GeV. The covariance increases from central to peripheral collisions for both positively and negatively charged particles. The right panel of figure 2 shows the covariance of v_3 and $A_{\rm ch}$, which remains approximately constant across centrality, in contrast to the v_2 -$A_{\rm ch}$ correlation. Figure 3 compares the normalized integral correlator difference (ΔIC/($\sigma^2_{A_{\rm ch}} v_n$)) as a function of collision centrality. The large difference between the normalized ΔIC values for v_2 and v_3 in the 0–20% centrality range arises from a finite ΔIC for v_3, together with the narrower $A_{\rm ch}$ distribution in central collisions. The observed agreement between the two, within uncertainties in the 20–70% centrality range, indicates the dominance of background effects, with little or no contribution from a CMW signal.

2.3 Search for an enhanced CMW signal in Ru+Ru collisions compared to Zr+Zr collisions

We carried out the CMW search in isobars, as the two nuclei were expected to have similar backgrounds due to their identical nucleon number, while the magnetic field, proportional to

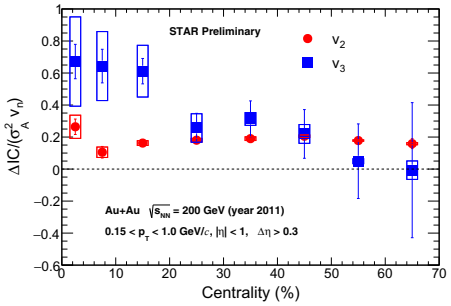

Figure 3. Comparison of normalized $\Delta IC/\sigma^2_{A_{ch}}$ for second and third harmonic as a function of collision centrality in Au+Au collisions at $\sqrt{s_{NN}}$ = 200 GeV.

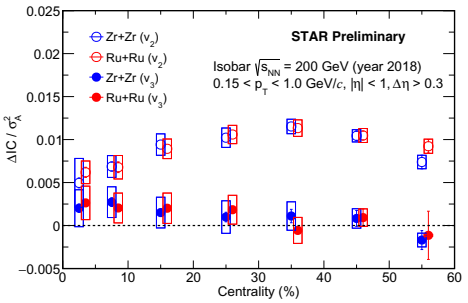

Figure 4. Comparison of $\Delta IC/\sigma^2_{A_{ch}}$ for both v_2 and v_3 as a function of collision centrality in Ru+Ru and Zr+Zr collisions at $\sqrt{s_{NN}}$ = 200 GeV. Markers are horizontally shifted for clarity.

the nuclear charge, would be more (∼10%) in Ru+Ru collisions compared to Zr+Zr collisions because of extra four protons in the former [11]. The large statistics isobar dataset provides an opportunity to place stringent constraints on the CMW signal contribution. Figure 4 presents the centrality dependence of $\Delta IC/\sigma^2_{A_{ch}}$ for both v_2 and v_3 in Zr+Zr and Ru+Ru collisions at $\sqrt{s_{NN}}$ = 200 GeV. For both harmonics, the results from the two systems are consistent within uncertainties, contrary to the expectation of an enhanced CMW signal in Ru+Ru collisions arising from the stronger magnetic field.

3 Summary

The CMW observable strength obtained with the spectator plane, which suppresses the elliptic flow background, is observed to be nearly independent of energy across the measured range. In addition, the signal extracted using the participant plane is larger compared to that extracted using spectator plane, and suggests dominance of background contributions in the CMW observable r_2. Furthermore, the integral correlator difference, $\Delta IC/(\sigma^2_{A_{ch}} v_n)$, for v_2 and v_3 in Au+Au collisions at 200 GeV are consistent within uncertainties, indicating no evidence of a CMW signal. Similarly, no enhanced CMW signal is observed in Ru+Ru collisions compared to Zr+Zr collisions at 200 GeV, despite the former having four additional protons.

References

[1] D. E. Kharzeev, L.D. McLerran, H.J. Warringa, Nucl. Phys. A **803**, 227 (2008).
[2] K. Fukushima, D. E. Kharzeev, H. J. Warringa, Phys. Rev. D **78**, 074033 (2008).
[3] D. T. Son, A. R. Zhitnitsky, Phys. Rev. D **70**, 074018 (2004).
[4] D. E. Kharzeev, H.-U. Yee, Phys. Rev. D **83**, 085007 (2011).
[5] Y. Burnier, D. E. Kharzeev, J. Liao, H.-U. Yee, Phys. Rev. Lett. **107**, 052303 (2011).
[6] D.E. Kharzeev, J. Liao, S.A. Voloshin, Prog. Part. Nucl. Phys. **88**, 1–28 (2016).
[7] L. Adamczyk et al. (STAR Collaboration), Phys. Rev. Lett. **114**, 252302 (2015).
[8] J. Adam et al. (ALICE Collaboration), Phys. Rev. C **193**, 044903 (2016)
[9] Hao-jie Xu, J. Zhao, Y. Feng, F. Wang, Phys. Rev. C **101**, 014913 (2020).

[10] A. Bzdak,P. Bozek, Phys. Lett. B **726**, 239 (2013).
[11] S. A. Voloshin, Phys. Rev. Lett. **105**, 172301 (2010).